CRYSTAL GROWTH & DESIGN

Article

pubs.acs.org/crystal

Crystal Structure Diversities Based on 4,4′-(2,3,6,7-Tetramethoxyanthracene-9,10-diyl)dibenzoic Acid: From 2D Layer to 3D Net Framework

Liangliang Zhang, Fuling Liu, Yu Guo, Xingpo Wang, Jie Guo, Yanhui Wei, Zhen Chen, and Daofeng Sun*

Key Lab of Colloid and Interface Chemistry, Ministry of Education, School of Chemistry and Chemical Engineering, Shandong University, Jinan, Shandong 250100, China

Supporting Information

ABSTRACT: Five metal−organic coordination complexes with the formulas of $\{Mn(L)(H_2O)_2\}_n$ (**1**), $\{[Cd_{1.5}L_{1.5}(DEF)_2]\cdot 2DEF\}_n$ (**2**), $[Co_{1.5}(L)_{1.5}(H_2O)]_n$ (**3**), $\{[Co(L)(H_2O)_2]\cdot 4H_2O\}_n$ (**4**), and $\{[Ni(L)(H_2O)_2]\cdot 4H_2O\}_n$ (**5**), (H_2L^{OMe} = 4,4′-(2,3,6,7-tetramethoxyanthracene-9,10-diyl)dibenzoic acid) based on a new rigid dicarboxylate ligand were synthesized and structurally characterized. Structural analysis reveals that H_2L^{OMe} acts as multibidentate bridging linker to connect metal ions and possesses similar coordination modes with terephthalic acid. Complex **1** is a (4^4)-sql layer incorporating bidentate-bridging H_2L^{OMe} and infinite Mn-$(CO_2)_2$ SBUs. Complexes **2** and **3** have similar 2D (3^6)-hxl layer topology structure based on bidentate-chelating/bridging H_2L^{OMe} ligand and trinuclear hourglass SBUs. Complexes **4** and **5** are isostructural and possess 3D open frameworks based on infinite M-(μ_2-H_2O) chain. From the viewpoint of crystal structure diversity and comparison, our results further demonstrate that the coordination mode of metal ions and ligand are the vital elements in determining the final crystal structure. Moreover, thermal stabilities of **1**−**5** and temperature-dependent photoluminescence behaviors of **1** and **2** are discussed.

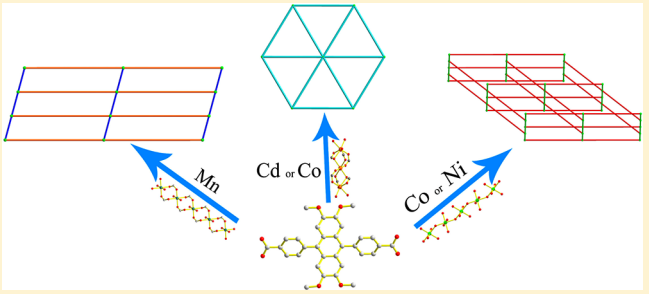

INTRODUCTION

The past decades have witnessed an explosive growth and evolution in metal−organic frameworks (MOFs), not only for their fascinating structural versatility but also for their potential functional properties, such as separation and gas storage, magnetism, luminescence, catalysis and recognition.[1−4] Generally, the construction of MOFs is seriously affected by the bewildering structure-directing factors such as the metal ions, the predesigned organic linkers, solvent, pH value of the solution, the temperature, the counterion with different bulk or coordination ability, the template and metal-to-ligand stoichiometry, etc.[5−7] Since design of rigid frameworks based on SBUs was successfully demonstrated for the first time in MOF-5, much more elaborate studies are required, which mainly focused on using the carboxylate functionality to chelate metal ions and lock them into rigid clusters. Recently, the coordination chemistry of terephthalic acid (H_2BDC) and its derivatives have been fully explored, which are illustrated with the synthesis of many functional BDC-based MOFs.

It is well-known that the substituent groups in the organic ligand, as well as the size of the ligand, have significant effects on the linking mode of the ligand, which further determine the structure of the product. Considering these in mind, we designed a new derivative of terephthalic acid, 4,4′-(2,3,6,7-tetramethoxyanthracene-9,10-diyl)dibenzoic acid (H_2L^{OMe}) (Scheme 1). In the H_2L^{OMe} molecule, the influence of methoxy substituent and enlargement in ligand length and width would exert on the solubility in polar and nonpolar solvents, the electron donor or acceptor effects, the hydrophobic character, and the possibility of

Scheme 1. Reaction Pathway of H_2L^{OMe}[a]

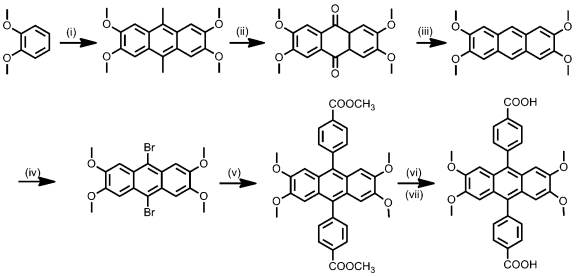

[a](i)MeCHO, H_2SO_4, −10 °C; (ii) $Na_2Cr_2O_7$, HAc reflux; (iii) Zn, NaOH 8−10% aq, 100 °C; (iv) Br_2,CCl_4 reflux; (v) (4-(methozycarbonyl)phenyl)boronic acid, $Pd(PPh_3)_4$, CsF, DMF, 90 °C; (vi) THF, MeOH; (vii) HCl, pH=1.

Received: September 26, 2012
Revised: October 31, 2012
Published: November 5, 2012

Table 1. Crystal Data for 1−5

compound	1	2	3	4	5
formula	$MnC_{32}H_{28}O_{10}$	$Cd_{1.5}C_{68}H_{80}N_4O_{16}$	$CoC_{32}H_{25.3}O_{8.7}$	$CoC_{32}H_{32}O_{13}$	$NiC_{32}H_{32}O_{11}$
M_r	627.48	1377.96	607.44	679.47	647.25
crystal system	triclinic	triclinic	trigonal	monoclinic	monoclinic
space group	$P\bar{1}$	$P\bar{1}$	$R\bar{3}$	$C2/c$	$C2/c$
a (Å)	4.6472(14)	15.489(2)	18.1473(10)	36.419(7)	36.622(10)
b (Å)	11.672(3)	16.205(2)	18.1473(10)	13.1869(19)	13.410(4)
c (Å)	13.455(4)	16.439(2)	36.182(4)	8.1455(19)	7.948(2)
α (deg)	90.036(4)	72.801(2)	90.00	90.00	90.00
β (deg)	97.870(5)	70.522(2)	90.00	100.045(4)	99.958(5)
γ (deg)	97.971(4)	68.048(2)	120.00	90.00	90.00
Z	1	2	9	4	4
V (Å^3)	715.8(4)	3538.3(8)	10319.2(14)	3852.0(13)	3844.5(18)
D_c (g cm^{-3})	1.456	1.293	0.880	1.172	1.181
μ (mm^{-1})	0.521	0.520	0.408	0.500	0.560
$F(000)$	325.0	1432	2823.0	1404.0	1424.0
no. of unique reflns	3545	12253	11185	9311	8940
no. of obsd reflns$[I > 2\sigma(I)]$	2942	7283	2429	3382	3380
parameters	394	808	192	213	216
GOF	1.032	1.143	1.094	1.080	1.042
final R	$R_1 = 0.0341$	$R_1 = 0.0543$	$R_1 = 0.0401$	$R_1 = 0.0494$	$R_1 = 0.0556$
indices $[I > 2\sigma(I)]^{a,b}$	$wR_2 = 0.0983$	$wR_2 = 0.1608$	$wR_2 = 0.1183$	$wR_2 = 0.1466$	$wR_2 = 0.1567$
R indices	$R_1 = 0.0379$	$R_1 = 0.0682$	$R_1 = 0.0488$	$R_1 = 0.0590$	$R_1 = 0.0784$
(all data)	$wR_2 = 0.1022$	$wR_2 = 0.1767$	$wR_2 = 0.1223$	$wR_2 = 0.1557$	$wR_2 = 0.1784$
largest difference peak and hole (e Å^{-3})	0.34 and −0.35	1.36 and −1.40	0.25 and −0.33	0.58 and −0.49	0.72 and −0.52

$^a R_1 = \sum||F_o| - |F_c||/\sum|F_o|$. $^b wR_2 = [\sum w(F_o^2 - F_c^2)^2/\sum w(F_o^2)^2]^{0.5}$.

additional intermolecular interactions and new coordination modes.

Solvothermal or conventional solution reactions of H_2L^{OMe} and metal ions resulted in the formation of five new metal−organic coordination complexes with different dimensions, $\{Mn(L^{OMe})(H_2O)_2\}_n$ (**1**), $\{[Cd_{1.5}L^{OMe}{}_{1.5}(DEF)_2]\cdot 2DEF\}_n$ (**2**), $[Co_{1.5}(L^{OMe})_{1.5}(H_2O)]_n$ (**3**), $\{[Co(L^{OMe})(H_2O)_2]\cdot 4H_2O\}_n$ (**4**), and $\{[Ni(L^{OMe})(H_2O)_2]\cdot 4(H_2O)\}_n$ (**5**). Complexes **1**−**5** were characterized by elemental analysis (EA), single-crystal X-ray crystallography, powder X-ray diffraction (PXRD), infrared spectroscopy (IR), and thermogravimtric analyses (TGA). In addition, luminescent properties of compounds **1**, **2**, and H_2L^{OMe} have also been investigated. Moreover, the coordination modes of the H_2L^{OMe} ligand as well as the comparisons and effects of the SBUs and metal ions on the structures of the complexes have also been discussed in detail.

EXPERIMENTAL SECTION

Materials and General Methods. H_2L^{OMe} was synthesized by a series of redox and Suzuki-couple reactions. The ^{1}H NMR in d^6-DMSO indicates the purity of the ligand [see Supporting Information]. Powder X-ray diffraction measurements were finished with a Bruker AXS D8 Advance. Elemental analyses (for C, H, or N) were carried out on a PerkinElmer 240 elemental analyzer. The FT-IR spectra were recorded in the range 4000−400 cm^{-1} on a Nicolet 330 FTIR Spectrometer using the KBr pellet method. Thermo-gravimetric analysis (TGA) experiments were performed using a PerkinElmer TGA 7 instrument (heating rate of 10 °C·min^{-1}; nitrogen stream). Photoluminescence spectra were measured on F-280 fluorescence spectrophotometer.

Preparation of Complexes 1−5. *$\{Mn(L)(H_2O)_2\}_n$ (**1**).* A mixture of $Mn(OAc)_2\cdot 4H_2O$ (12 mg, 0.05 mmol) and H_2L^{OMe} (10 mg, 0.02 mmol) was dissolved in NMP (*N*-methyl pyrrolidone)/DMA (dimethylacetamide)/H_2O mixed solvent (1 mL, *v*/*v*/*v* 1/1/1). Then, the solution was sealed in a pressure-resistant glass tube, slowly heated to 130 °C from room temperature in 600 min, kept at 130 °C for 3000 min, and then slowly cooled to 30 °C in 800 min. The light-yellow crystals that formed were collected and dried in the air. (Yield: 57%, based on manganese.) Anal. Calcd. (found) for $MnC_{32}H_{28}O_{10}$: C, 60.91 (61.25); H, 4.62 (4.50) %. IR (KBr): ν(cm^{-1}) = 3505 (s), 2953 (w), 2828 (w), 1639 (m), 1540 (m), 1493 (w), 1389 (w), 1240 (w), 1119 (s), 851 (w), 750 (w), 462 (w).

*$\{[Cd_{1.5}L_{1.5}(DEF)_2]\cdot 2DEF\}_n$ (**2**).* A mixture of $Cd(NO_3)_2\cdot 4H_2O$ (15 mg, 0.05 mmol) and H_2L^{OMe} (10 mg, 0.02 mmol) was dissolved in 1 mL DEF (diethylforamide). Then, the solution was sealed in a pressure-resistant glass tube, slowly heated to 90 °C from room temperature in 300 min, kept at 90 °C for 3000 min, and then slowly cooled to 30 °C in 600 min. The yellowish block crystals that formed were collected and dried in the air. (Yield: 51%, based on cadmium.) Anal. Calcd. (found) for $Cd_{1.5}C_{68}H_{80}N_4O_{16}$: C, 58.70 (59.27); H, 5.98 (5.85); N, 4.24 (4.07) %. IR (KBr): ν(cm^{-1}) = 3470 (m), 2973 (m), 2830 (w), 1654 (s), 1603 (s), 1531 (m), 1492 (s), 1435 (s), 1237 (s), 1207 (m), 1118 (s), 1036 (w), 966 (w), 850 (m), 749 (m), 583 (m), 535 (w), 486 (w).

*$[Co_{1.5}(L)_{1.5}(H_2O)]_n$ (**3**).* A mixture of $Co(NO_3)_2\cdot 6H_2O$ (15 mg, 0.05 mmol) and H_2L^{OMe} (10 mg, 0.02 mmol) was dissolved in 1 mL DMA. Then, the solution was sealed in a pressure-resistant glass tube, slowly heated to 120 °C from room temperature in 300 min, kept at 120 °C for 3000 min, and then slowly cooled to 30 °C in 600 min. The purple block crystals that formed were collected and dried in the air. (Yield: 41%, based on cobalt.) Anal. Calcd. (found) for $Co_{1.5}C_{48}H_{38}O_{13}$: C, 67.40 (67.64); H, 4.38 (4.49) %. IR (KBr): ν(cm^{-1}) = 3448 (s), 2936 (w), 2827 (w), 1636 (s), 1545 (m), 1492 (s), 1387 (s), 1237 (s), 1204 (m), 1117 (m), 1018 (m), 899 (w), 845 (m), 747 (m), 714 (m), 580 (m), 536 (m).

*$\{[Co(L)(H_2O)_2]\cdot 4H_2O\}_n$ (**4**).* Compound **4** was prepared by liquid diffusion method. A mixture of H_2L^{OMe} (20 mg, 0.05 mmol) and H_2O (5 mL) was stirred, 1 mol/L KOH solution was dropped into the mixture to give a clear solution, then the mixed solution was carefully added into the bottom of a 18 × 180 mm test tube; after that, $Co(NO_3)_2\cdot 6H_2O$ (15 mg, 0.05 mmol) in 10 mL of ethanol was carefully layered onto the solution. The resulting mixture was kept at room temperature, and yellow crystals were obtained after three weeks. (Yield: 50%, based on cobalt.) Anal. Calcd. (found) for $CoC_{32}H_{28}O_{13}$: C, 56.38 (56.56); H, 4.47 (4.15); N, 11.46 (11.41) %. IR (KBr): ν(cm^{-1}) = 3489 (w), 1605

dx.doi.org/10.1021/cg301403w | *Cryst. Growth Des.* 2012, 12, 6215−6222

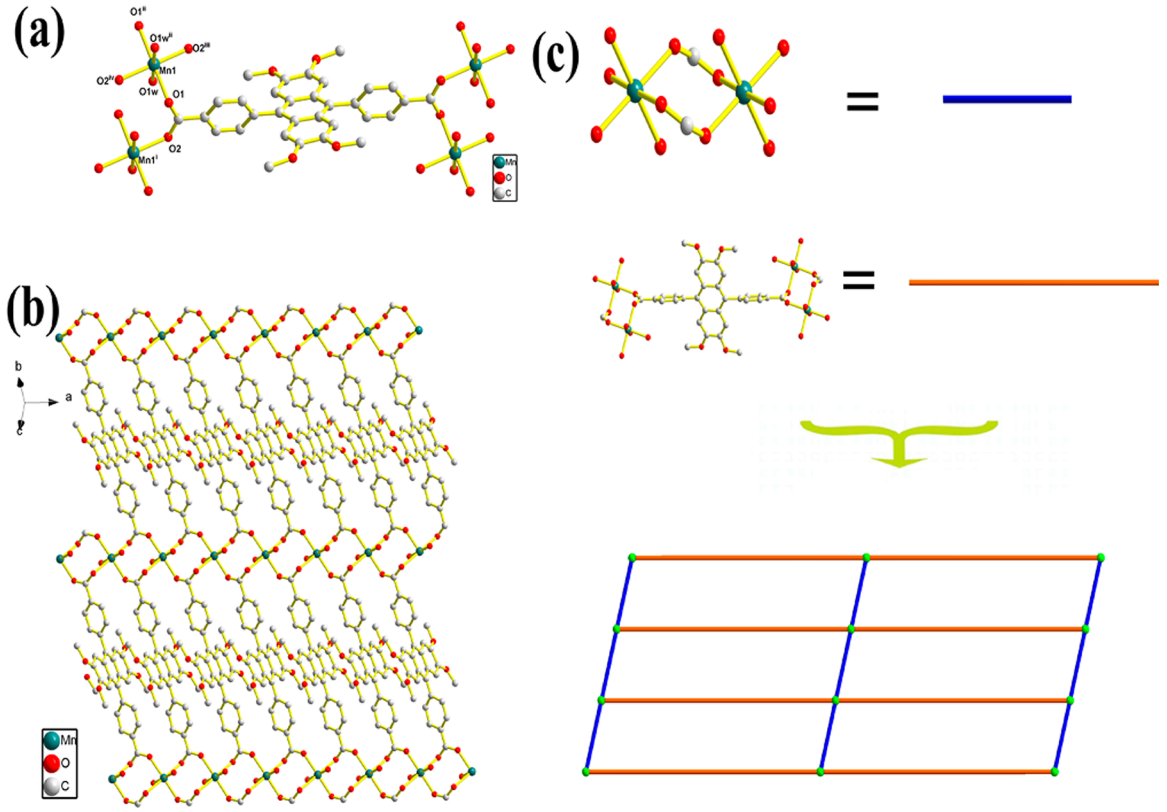

Figure 1. (a) Coordination environment of the Mn(II) ion and the linkage mode of ligand in **1**. Hydrogen atoms are omitted for clarity. (b) The 2D layer linked by binuclear Mn SBU. (c) Schematic representation of the (4^4)-sql layer connected topology (symmetry code: (i) $-x+1, y, z$; (ii) $-x+1, 1-y, 1-z$; (iii) $1+x, y, z$; (iv) $-x, 1-y, 1-z$).

(m), 1530 (s), 1492 (s), 1433 (s), 1401 (s), 1238 (s), 1206 (m), 1120 (s), 1018 (m), 845 (m), 750 (s), 584 (m), 537 (w), 490 (w).

{[Ni(L)(H$_2$O)$_2$]·4H$_2$O}$_n$ (***5***). The preparation of **5** was similar to that of **4** except that Ni(NO$_3$)$_2$·6H$_2$O (25 mg, 0.1 mmol) was used instead of Co(NO$_3$)$_2$·6H$_2$O. The yellow crystals of **5** were obtained in a 44% yield based on nickel. Anal. Calcd. (found) for NiC$_{32}$H$_{28}$O$_{11}$: C, 59.38 (59.38); H, 4.47 (4.36) %. IR (KBr): ν(cm^{-1}) = 3422 (w), 1565 (m), 1494 (s), 1435 (s), 1384 (s), 1239 (s), 1119 (m), 1018 (m), 845 (m), 751 (m), 584 (w), 536 (w).

X-ray Crystallography. Single crystals of the compounds **1**−**5** with appropriate dimensions were chosen under an optical microscope and quickly coated with high vacuum grease (Dow Corning Corporation) before being mounted on a glass fiber for data collection. Data were collected on a Bruker Apex II Image Plate single-crystal diffractometer with graphite-monochromated Mo Kα radiation source (λ = 0.71073 Å) operating at 50 kV and 30 mA for **1**−**5**. All absorption corrections were applied using the multiscan program SADABS. In all cases, the highest possible space group was chosen. All structures were solved by direct methods using SHELXS-97[8] and refined on F^2 by full-matrix least-squares procedures with SHELXL-97.[9] Atoms were located from iterative examination of difference F-maps following least-squares refinements of the earlier models. Hydrogen atoms were placed in calculated positions and included as riding atoms with isotropic displacement parameters 1.2 times U_{eq} of the attached C atoms. All structures were examined using the Addsym subroutine of PLATON[10] to ensure that no additional symmetry could be applied to the models. The crystallographic details of **1**−**5** are summarized in Table 1. Selected bond lengths and angles for **1**−**5** are collected in Table S1 (Supporting Information). The hydrogen bond geometries for **1**−**5** are shown in Table S2 (Supporting Information).

RESULT AND DISCUSSION

Syntheses. Compounds **1**−**3** were synthesized by the reaction of M(NO$_3$)$_2$ or M(OAc)$_2$ and H$_2$L^{OMe} through solvothermal method in a glass tube heated in a programmed oven. The syntheses of complexes **4** and **5** were carried out through a conventional diffusion method in a test tube at room temperature.

Descriptions of the Crystal Structures. *{Mn(L)(H$_2$O)$_2$}$_n$* (***1***). X-ray crystallographic analysis revealed that **1** crystallizes in triclinic $P\bar{1}$ space group. There is half manganese(II) atom, half L^{OMe} ligand, and one coordinated water molecule in the asymmetric unit. As illustrated in Figure 1a, the six-coordinated Mn(II) adopts distorted [MnO$_6$] octahedron geometry, where four O atoms come from carboxylic group oxygen atoms (O1, O1^{ii}, O2, O2^{ii}) of four L^{OMe} ligands and the other two oxygen atoms (O1w, O1w^{ii}) are from two coordinated water molecules. In compound **1**, L^{OMe} ligand adopts μ_2 bridging fashion. The infinite binuclear Mn$_2$(CO$_2$)$_2$ SBUs and linear L^{OMe} ligand give the 2D layer coordination network, as shown in Figure 1b.The Mn−O distance range from 2.1551(14) to 2.2198(14) Å, and the distance of Mn−Ow is 2.1867(15) Å, respectively. The neighbor Mn ions distances are 4.64(7) Å. All the bond distances and angles are comparable to those observed in other Mn (II) complexes [11] (symmetry code: (i) $-x+1, y, z$; (ii) $-x+1, 1-y, 1-z$; (iii) $1+x, y, z$; (iv) $-x, 1-y, 1-z$).

To get better insight into the framework, its topological analysis is carried out. If the infinite binuclear Mn cations and L^{OMe} ligand are considered as linear linkers, the structure of compound **1** can be symbolized as a typical (4^4)-sql layer (Figure 1c).[12] The 2D layers of compound **1** are further connected by the weak intermolecular and intramolecular O−H···O interactions to result in a 3D supramolecular framework.

{[Cd$_{1.5}$L$_{1.5}$(DEF)$_2$]·2DEF}$_n$ (***2***). X-ray single-crystal diffraction reveals that complex **2** has a 2D framework with the trinuclear

dx.doi.org/10.1021/cg301403w | *Cryst. Growth Des.* 2012, 12, 6215−6222

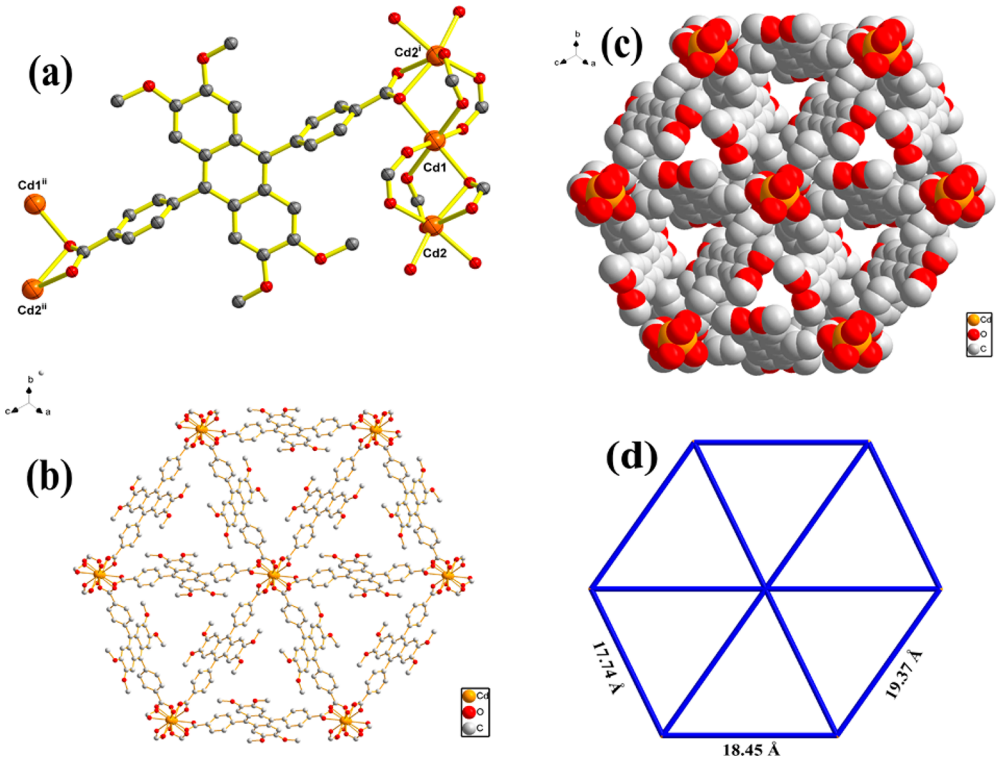

Figure 2. (a) Coordination environment of the Cd(II) ion and the linkage mode of ligand in **2**. Hydrogen atoms are omitted for clarity. (b) The 2D ball and stick mode of structure **2**. (c) The 2D space-filling mode of structure **2**. (d) Schematic representation of the (3^6)-hxl layer connected topology (symmetry codes: (i) $-x + 1, 1 - y, -z + 1$; (ii) $-x + 1, y + 1, z$).

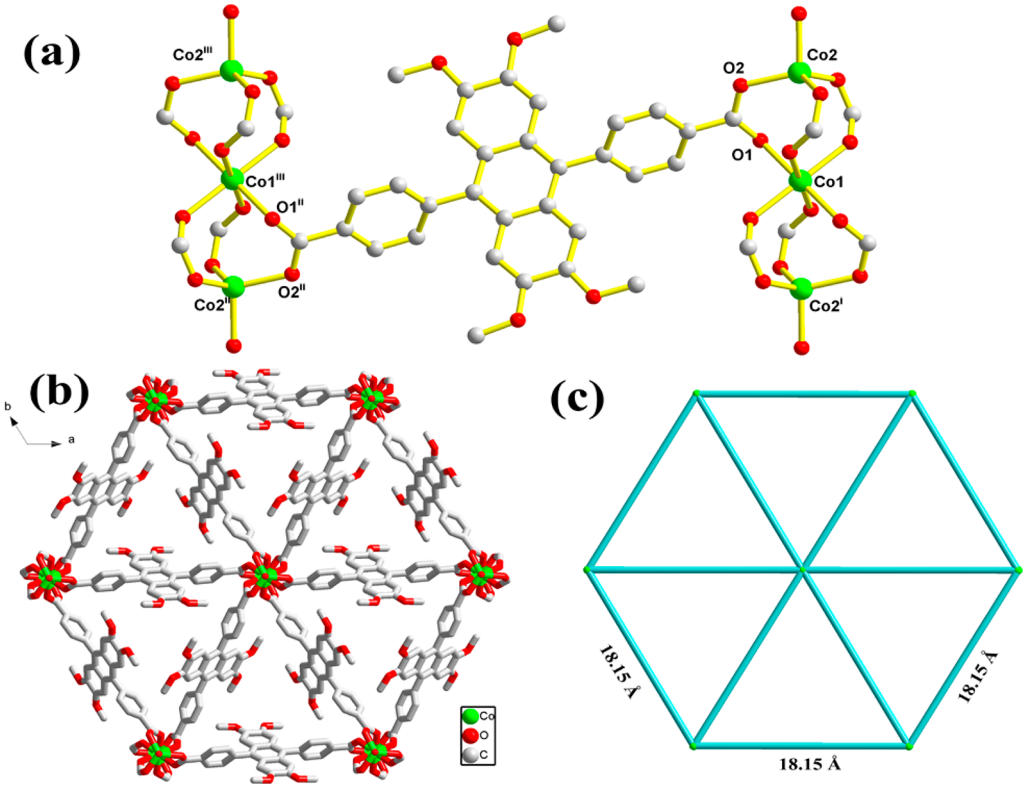

Figure 3. (a) Coordination environment of the Co (II) ion and the linkage mode of ligand in **3**. Hydrogen atoms are omitted for clarity. (b) The 2D wire/stick mode of structure **3**. (c) Schematic representation of the (3^6)-hxl layer connected topology (symmetry codes: (i) $-x, -y, -z$; (ii) $-x + 1, -y, -z$; (iii) $1 + x, y, z$).

dx.doi.org/10.1021/cg301403w | *Cryst. Growth Des.* 2012, 12, 6215−6222

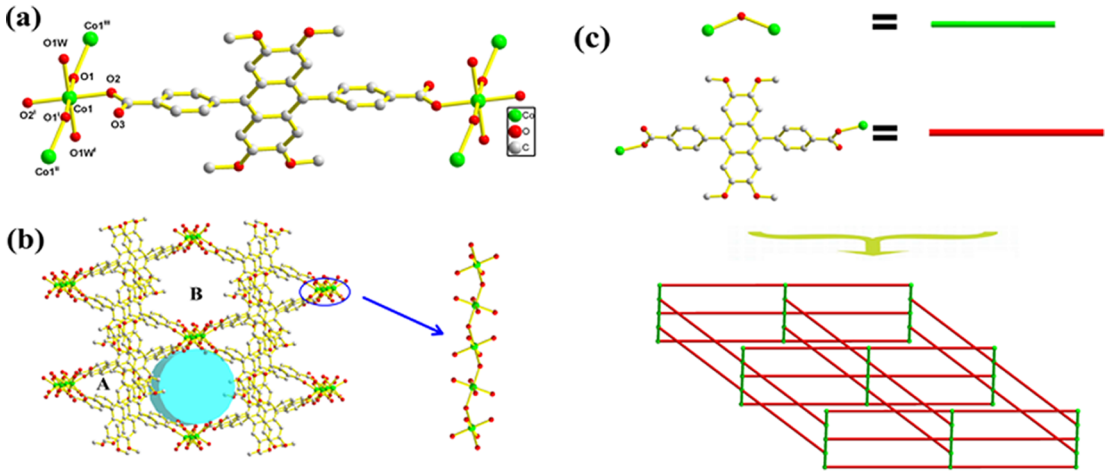

Figure 4. (a) Coordination environment of the Co(II) ion and the linkage mode of ligand in **4** (symmetry codes: (i) $-x, -y+2, -z$; (ii) $-x, y, -z-1/2$; (iii) $-x, y, -z+1/2$.). Hydrogen atoms are omitted for clarity. (b) The 3D net structure of **4**. (c) Schematic representation of topology.

hourglass cadmium clusters as the secondary building unit, in which, trinuclear cadmium possess centrosymmetric structure and Cd1 is the center of symmetry. Complex **2** crystallized in triclinic $P\bar{1}$ space group. The asymmetrical unit of **2** contains one dependent Cd2(II) atom, half Cd1(II) atom, one and a half $\mathbf{L}^{OMe}$ ligands, two coordinated DEF molecules, and two lattice DEF molecules. Coordinated DEF molecules occupy the coordinate sites of central metal ions, which interrupts to construct high-dimensional architectures. The coordination environments of two Cd(II) atoms are shown in Figure 2a. The carboxylate group in compound **2** adopts two kinds of coordination modes, one adopts bridging-chelating/bridging-chelating coordination mode, while the other adopts bis-bridging coordination mode. Cd1 is six-coordinated by six carboxylate oxygen atoms (Cd1−O4 2.337 (3), Cd1−O7 2.204 (3), and Cd1−O10 2.260 (3) Å) from four $\mathbf{L}^{OMe}$ ligands, forming an octahedron geometry. The Cd−O distance ranges from 2.204(3) to 2.337(3) Å. Cd2 has similar coordination environment and six-coordinated in a slightly distorted octahedron geometry by four carboxylate oxygen atoms from three $\mathbf{L}^{OMe}$ ligands and two oxygen atoms from coordinated DEF molecules, respectively. The Cd−O distance ranges from 2.196(4) to 2.386(3) Å, which are similar to those of other reported Cd(II) complexes.[13]

The topological analysis of complex **2** has been performed. The individual 2-dimensional layer-like motif (Figure 2b,c) with the Schläfli symbol of $3^6{\cdot}4^6{\cdot}5^3$ represents a 6-connected topology type (Figure 2d).[14] In this case, the trinuclear hourglass cadmium (SBU) is simplified as the 6-connected node and the $H_2\mathbf{L}^{OMe}$ ligand as a linker. The distances between nodes are 17.74, 18.45, and 19.37 Å, respectively. In compound 2, the 2D layer stuck to give rise a 3D supramolecular architecture because of weak layer-to-layer H bonds and C−H$\cdots\pi$ interactions.

$[Co_{1.5}(L)_{1.5}(H_2O)]_n$ ***(3)***. X-ray single crystal diffraction reveals that complex **3** has a similar 2D framework with complex **2**. In compound **3**, trinuclear hourglass With cobalt clusters as the secondary building unit, trinuclear Co posse's centrosymmetric structure and Co1 is the center of symmetry. Complex **3** crystallized in trigonal $R\bar{3}$ space group. Analysis of the local symmetry shows that both Co1 and Co2 reside on the crystallographic 3-fold axis; at the same time, Co1 located in the center of inversion. The asymmetrical unit of **3** contains one-sixth Co1(II) atom, one-third Co2(II) atom, a half $\mathbf{L}^{OMe}$ ligand, and one-third coordinated water molecular. Coordinated water molecule occupies the coordinate sites of central metal ions, which interrupts to construct high-dimensional architectures. The coordination environments of two Co(II) atoms are shown in Figure 3a. Co1 is six-coordinated by six carboxylate oxygen atoms (Co1−O1 2.078(2) Å) from six $\mathbf{L}^{OMe}$ ligands, forming a octahedron geometry. Co2 is four-coordinated in a slightly distorted terahedron geometry by three carboxylate oxygen atoms (Co2−O2 1.958(2) Å) from three $\mathbf{L}^{OMe}$ ligands and one oxygen atom from coordinated water molecule, respectively. The Co−Ow distance is 2.006(4) Å. All the bond distances and angles are comparable to those observed in another Co(II) complex.[15] The carboxylate group in compound **3** adopts μ_2-η^1:η^1 mode to link two trinuclear Co(II) parts, which results in the final 2D layer structure (Figure 3b).

The topological analysis of complex **3** has also been performed. Complex **3** has a similar 2D (3^6)-hxl layer framework with complex **2**, but the distance of SBUs node is 18.15 Å only, which is different from **2** (Figure 3c). That means the arrangement of L^{2-} in 3 is more regular than that in **2**.

$\{[Co(L)(H_2O)_2]{\cdot}4H_2O\}_n$ (4) and $\{[Ni(L)(H_2O)_2]{\cdot}4H_2O\}_n$ ***(5)***. Single-crystal X-ray analysis of **4** and **5** indicates that they are isostructural, so the structure of **4** is described representatively here in detail. Compound **4** is a three-dimensional framework and crystallizes in monoclinic $C2/c$ space group. The asymmetric unit contains half Co(II) ion, half $H_2\mathbf{L}^{OMe}$ ligand, one lattice water molecule, one coordinated water molecule, and one protonated water molecular. As illustrated in Figure 4a, the six-coordinated Co(II) adopts distorted $[CoO_6]$ octahedron geometry, where two O atoms come from two different $\mathbf{L}^{OMe}$ ligands, two oxygen atoms are from two coordinated water molecules, and the other two oxygen atoms are from two deprotonated oxygen atoms. In compound **4**, each $\mathbf{L}^{OMe}$ ligand adopts μ_2-η^1 bridging fashion. The Co−O and Co−Ow distance are 2.0423(16) and 2.0601(19) Å, respectively. The average Co−O distance is 2.2166(10) Å. So the whole 3D crystal structure of **4** can be thought that 1D infinite Co−O chains were connected by linear $\mathbf{L}^{OMe}$ ligand (Figure 4b).

There exist two kinds of channels in **4**: one is triangle marked as A; the other is a hexagon marked as B, and it is explicit that B is much bigger than A with 23.2% solvent-accessible volume calculated from PLATON. Each A is surrounded by three A and B; every B is connected by six A viewed along c directions. The dimensions of triangle channel A is 16.5 × 7.2 × 13.2 Å and

dx.doi.org/10.1021/cg301403w | *Cryst. Growth Des.* 2012, 12, 6215−6222

hexagon channel B is 16.5 × 8.4 × 10.2 Å, respectively, and the content of B are full of water molecules. Topologically, a three-dimensional net topology is found by connecting infinite SBUs and linear L^{OMe} ligand (Figure 4c).

Comparison of the Crystal Structures. Single-crystal X-ray diffraction analyses reveal that complexes **1**−**5** exhibit structural diversity from 2D layer to 3D net framework. From the structural point of view, the rich structures maybe partly attributed to the versatile coordination modes of L^{OMe} anions, and the coordination modes of L^{OMe} are listed in Scheme 2.

Scheme 2. Coordinate Mode of L^{OMe} in 1−5

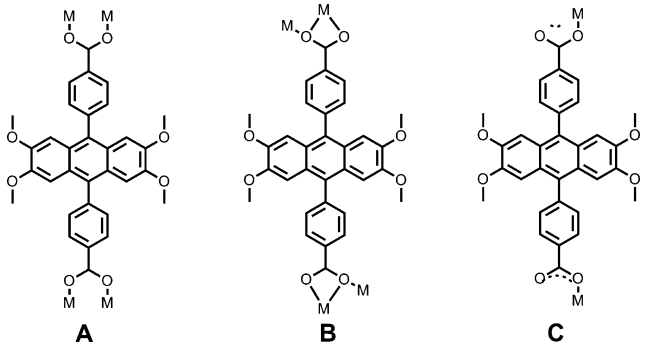

Among these modes, mode A appears in **1** and **3**, mode C is observed in **4** and **5**, while L^{OMe} in **2** adopts mode A and B. Comparing **1** with **3**, though both **1** and **3** adopt mode A, they possess different 2D topologies, (4^4)-sql layer vs (3^6)-hxl layer, which may derive from the existence of different SBUs in **1** and **3**. In **1**, the carboxylate groups connect Mn^{2+} ions to generate an infinite SBU, and the backbone of L^{OMe} adopt the same arrangement as the linkers to connect the 1D SBUs to form the final (4^4) layer. The two coordinated water molecules in each Mn^{2+} ion prevent its further extension to form high-dimensional framework. However, in **3**, the carboxylate groups connect Co^{2+} to form a trinuclear hourglass SBU, and the backbone of L^{OMe} can link the SBU from six directions in [110] plane to generate a $(3^6{\cdot}4^6{\cdot}5^3)$ layer. A similar result is found in complex **2**, but the hourglass SBU is slightly different than that in **3**. The component of hourglass SBU is $Co_3C_6O_{14}$ in **3** and $Cd_3C_6O_{16}$ in **2**, respectively.

Complexes **4** and **5** were synthesized in a conventional diffusion method at room temperature. As known, the coordination competition with central metal ions between carboxylate group and water is drastic in solution at room temperature. As a result, the L^{OMe} ligand adopts C coordination mode to link two metal ions, and there are two terminal water ligands and two bridging water ligands in each metal ion. The bridging water ligands connect the metal ions to form an infinite SBU. Different from complex **1** that the backbone of L^{OMe} adopts the same arrangement and connect the SBU in the same direction, the backbone of L^{OMe} in complexes **4** and **5** link the 1D SBU in different directions to generate the final 3D open framework.

IR Spectra, X-ray Powder Diffraction Analyses, and Thermal Analyses. The IR spectra (Figure S1, Supporting Information) of compounds **1**, **3**, **4**, and **5** show broad peak at 3500 cm^{-1} attributed to the O−H stretching vibration of the coordinated water molecules, and the sharp bands in the ranges of 1700−1600 and 1400−1300 cm^{-1} are attributed to asymmetric and symmetric stretching vibrations of carboxylic group, respectively. Powder X-ray diffraction (XRD) has been used to check the phase purity of the bulky samples in the solid state. For compounds **1**−**5**, the measured XRD patterns closely match the simulated patterns generated from the results of single-crystal diffraction data (Figure S2, Supporting Information), indicative of pure products. The dissimilarities in intensity may be due to the preferred orientation of the crystalline powder samples.

The TG analysis was performed in N_2 atmosphere on compounds **1**−**5** (Figure S3, Supporting Information). In five compounds, only **5** has three identifiable weight loss steps, and the other four compounds have only two weight loss steps. However, the initial decomposition temperatures of **1**−**5** are obviously different from each other. For compound **1**, the first weight loss in the temperature of 162 °C is consistent with the removal of coordinated water molecule (obsd 5.6%; calcd 5.8%). The second weight loss from 162 to 590 °C is attributed to the collapse of the framework of **1**. For **2**, the first weight loss in the temperature of 213 °C is consistent with the removal of lattice and coordinated DEF molecule (obsd 28.9%; calcd 29.3%). The second weight loss from 213 to 545 °C is attributed to the collapse of the framework of **2**. The remaining residue corresponds to the formation of CdO (obsd 13.9%; calcd 13.2%). For **3**, the first weight loss in the temperature range of 30−210 °C is consistent with the removal of a coordinated water molecule (obsd 10.6%; calcd 11.4%). The second weight loss from 210 to 423 °C is attributed to the collapse of the framework of **3**. For **4**, the first weight loss in the temperature range of 30−87 °C is consistent with the removal of a lattice water molecule (obsd 15.4%; calcd 14.9%). The second weight loss from 87 to 496 °C is attributed to the collapse of the framework of **4**. For **5**, the first weight loss in the temperature range of 30−80 °C is consistent with the removal of a lattice water molecule (obsd 16.8%; calcd 17.1%). The second weight loss from 80 to 273 °C is attributed to the removal of a lattice water molecule (obsd 7.2%; calcd 7.7%). The third weight loss from 273 to 590 °C is attributed to the collapse of the framework of **5**.

Photoluminescence Properties. Because of luminescent properties of d^{10} transition metal and their various applications in chemical sensors, photochemistry, and electroluminescent display, luminescence coordinated compounds are of great current interest.[16] Thus, the photoluminescence spectrum of **1**, **2**, and H_2L^{OMe} were investigated intensively at room temperature (298 K) and in low temperature (77 K). As shown in Figure 5,

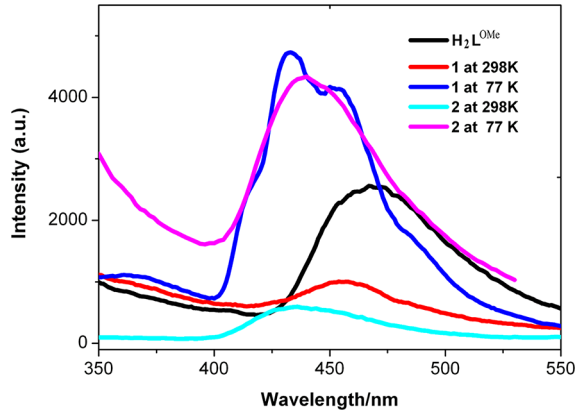

Figure 5. Temperature-dependent photoluminescences of free ligand and compounds **1** and **2**.

dx.doi.org/10.1021/cg301403w | *Cryst. Growth Des.* 2012, 12, 6215−6222

the free ligand H_2L^{OMe} displays photoluminescence with emission maxima at 467 nm upon 280 nm excitation, which can be attributed to the $\pi^*\cdots\pi$ transition of the p electrons of the aromatic rings. Complex **1** displays luminescent emission bands at 458 nm (λ_{ex} = 310 nm) at 298 K; complex **1** shows blue-shifted (Δ = 9 nm) photoluminescence with respect to H_2L^{OMe} at 298 K. When cooling from 298 to 77 K, the emission band of complex **1** blue-shifted 34 to 433 nm (λ_{ex} = 310 nm) accompanying the dramatic enhancement in intensity. As for complex **2**, its emission maxima locates at 436 nm at 298 K; when cooling to 77 K, the emission band of complex 2 blue-shifted 37 to 440 nm (λ_{ex} = 280 nm); also accompanying the dramatic enhancement in intensity. The emission of complex **2** is neither metal-to-ligand charge transfer nor ligand-to-metal charge transfer.[17] Because the Cd(II) ion is difficult to oxidize or to reduce due to its d^{10} electronic configuration. The increase in fluorescence can be attributed to the rigidity of ligands, which is favorable for cold conditions, with the decrease of radiationless decay process of the intraligand ($\pi \rightarrow \pi^*$) excited state and effect of intramolecular or intermolecular interactions among organic linkers.[18]

CONCLUSIONS

A series of metal−organic coordination complexes based on a new rigid dicarboxylate ligand were synthesized and characterized. These complexes show diverse structures and dimensionalities from 2D (4^4)-sql layer (**1**) to 2D (3^6)-hxl layer (**2**,**3**) to 3D net (**4**,**5**). The diversities of structures result from the various SBUs with different geometries, coordinative abilities, and sizes, which induce the different coordination spheres of central metal ions and different arrangements and coordination fashions of L^{OMe} ligand. Additionally, complexes **1**−**5** display modest thermal stability, and **1** and **2** show strong temperature-dependent photoluminescent emission.

ASSOCIATED CONTENT

Supporting Information

Crystallographic data in CIF format, additional figures of the structures, hydrogen-bonding geometries, powder X-ray diffraction (PXRD) patterns, TGA, and IR spectra for **1**−**5**. This material is available free of charge via the Internet at http://pubs.acs.org.

AUTHOR INFORMATION

Corresponding Author

*Fax: +86-531-88364218. E-mail: dfsun@sdu.edu.cn.

Notes

The authors declare no competing financial interest.

ACKNOWLEDGMENTS

This work was supported by the NSFC (National Natural Science Foundation of China) (Grant No. 90922014), the Shandong Natural Science Fund for Distinguished Young Scholars (JQ201003), and Independent Innovation Foundation of Shandong University (2010JQ011).

REFERENCES

(1) (a) Rowsell, J. L. C.; Yaghi, O. M. *Angew. Chem., Int. Ed.* **2005**, *44*, 4670−4679. (b) Sun, D.; Yang, C.-F.; Xu, H.-R.; Zhao, H.-X.; Wei, Z.-H.; Zhang, N.; Yu, L.-J.; Huang, R.-B.; Zheng, L.-S. *Chem. Commun.* **2010**, *46*, 8168−8170. (c) Dinca, M.; Dailly, A.; Liu, Y.; Brown, C. M.; Neumann, D. A.; Long, J. R. *J. Am. Chem. Soc.* **2006**, *128*, 16876−16883. (d) Sun, D.; Luo, G.-G.; Zhang, N.; Huang, R.-B.; Zheng, L.-S. *Chem. Commun.* **2011**, *47*, 1461−1463. (e) Ma, S.-Q.; Sun, D.-F.; Wang, X.-S.; Zhou, H.-C. *Angew. Chem., Int. Ed.* **2007**, *46*, 2458−2462.

(2) (a) Sato, O. *Acc. Chem. Res.* **2003**, *36*, 692−700. (b) Gao, E.-Q.; Yue, Y.-F.; Bai, S.-Q.; He, Z.; Yan, C.-H. *J. Am. Chem. Soc.* **2004**, *126*, 1419−1426. (c) Wang, X.-Y.; Wang, Z.-M.; Gao, S. *Chem. Commun.* **2008**, *3*, 281−294. (d) Sun, D.; Zhang, L.; Yan, Z.; Sun, D. *Chem. Asian J.* **2012**, *7*, 1558−1561. (e) Cheng, X.-N.; Zhang, W.-X.; Lin, Y.-Y.; Zheng, Y.-Z.; Chen, X.-M. *Adv. Mater.* **2007**, *19*, 1494−1498. (f) Sun, D.; Liu, F.-J.; Huang, R.-B.; Zheng, L.-S. *Inorg. Chem.* **2011**, *50*, 12393−12395.

(3) (a) Cariati, E.; Pizzotti, M.; Roberto, D.; Tessore, F.; Ugo, R. *Coord. Chem. Rev.* **2006**, *250*, 1210−1233. (b) Evans, O. R.; Lin, W. B. *Chem. Mater.* **2001**, *13*, 2705−2712. (c) Sun, D.; Wang, D.-F.; Han, X.-G.; Zhang, N.; Huang, R.-B.; Zheng, L.-S. *Chem. Commun.* **2011**, *47*, 746−748.

(4) (a) Yoshizawa, M.; Tamura, M.; Fujita, M. *Science* **2006**, *312*, 251−254. (b) Rosi, N. L.; Eckert, J.; Eddaoudi, M.; Vodak, D. T.; Kim, J.; O'Keeffe, M.; Yaghi, O. M. *Science* **2003**, *300*, 1127−1129. (c) Seo, J. S.; Whang, D.; Lee, H.; Jun, S. I.; Oh, J.; Jeon, Y. J.; Kim, K. *Nature* **2000**, *404*, 982−968. (d) Zhao, D.; Yuan, D.-Q.; Sun, D.-F.; Zhou, H.-C. *J. Am. Chem. Soc.* **2009**, *131*, 9186−9188. (e) Zhou, W.; Wu, H.; Yildirim, T. *J. Am. Chem. Soc.* **2008**, *130*, 15268−15269. (f) Farrusseng, D.; Aguado, S.; Pinel, C. *Angew. Chem., Int. Ed.* **2009**, *48*, 7502−7513. (g) Evans, O. R.; Lin, W. *Acc. Chem. Res.* **2002**, *35*, 511−522. (h) Zou, R.-Q.; Sakurai, H.; Xu, Q. *Angew. Chem., Int. Ed.* **2006**, *45*, 2542−2546. (h) Wu, C.-D.; Lin, W. *Angew. Chem., Int. Ed.* **2005**, *44*, 1958−1961. (i) Cho, S. H.; Ma, B. Q.; Nguyen, S. T.; Hupp, J. T.; Albrecht-Schmitt, T. E. *Chem. Commun.* **2006**, *24*, 2563−2565. (j) Chen, B.-L.; Xiang, S. C.; Qian, G.-D. *Acc. Chem. Res.* **2010**, *43*, 1115−1124.

(5) (a) Roland, B. K.; Carter, C.; Zheng, Z. P. *J. Am. Chem. Soc.* **2002**, *124*, 6234−6235. (b) Sun, D.; Wei, Z. H.; Yang, C. F.; Wang, D. F.; Zhang, N.; Huang, R. B.; Zheng, L. S. *CrystEngComm* **2011**, *13*, 1591−1601. (c) Yang, J.; Ma, J. F.; Liu, Y. Y.; Ma, J. C.; Batten, S. R. *Inorg. Chem.* **2007**, *46*, 6542−6555. (d) Sun, D.; Li, Y.-H.; Hao, H.-J.; Liu, F.-J.; Zhao, Y.; Huang, R.-B.; Zheng, L.-S. *CrystEngComm* **2011**, *13*, 6431−6441. (e) Chen, H.-C.; Hu, H.-L.; Chan, Z. K.; Yeh, C. W.; Jia, H.-W.; Wu, C.-P.; Chen, J.-D.; Wang, J.-C. *Cryst. Growth Des.* **2007**, *7*, 698−704. (f) Sun, D.; Wang, D. F.; Liu, F. J.; Hao, H. J.; Zhang, N.; Huang, R. B.; Zheng, L. S. *CrystEngComm* **2011**, *13*, 2833−2836. (g) Lang, J.-P.; Xu, Q.-F.; Yuan, R.-X.; Abrahams, B. F. *Angew. Chem., Int. Ed.* **2004**, *43*, 4741−4745.

(6) (a) Rispens, M. T.; Meetsma, A.; Rittberger, R.; Brabec, C. J.; Sariciftci, N. S.; Hummelen, J. C. *Chem. Commun.* **2003**, *17*, 2116−2118. (b) Sun, D.; Wang, D.-F.; Zhang, N.; Liu, F.-J.; Hao, H.-J.; Huang, R.-B.; Zheng, L.-S. *Dalton Trans.* **2011**, *40*, 5677−5679. (c) Chen, Y.; Li, H. X.; Liu, D.; Liu, L.-L.; Li, N.-Y.; Ye, H.-Y.; Zhang, Y.; Lang, J.-P. *Cryst. Growth Des.* **2008**, *8*, 3810−3816. (d) Sun, D.; Xu, Q.-J.; Ma, C.-Y.; Zhang, N.; Huang, R.-B.; Zheng, L.-S. *CrystEngComm* **2010**, *12*, 4161−4167. (e) Tong, M.-L.; Zheng, S.-L.; Chen, X.-M. *Chem.—Eur. J.* **2000**, *6*, 3729−3738.

(7) (a) Zheng, P. Q.; Ren, Y. P.; Long, L.-S.; Huang, R.-B.; Zheng, L.-S. *Inorg. Chem.* **2005**, *44*, 1190−1192. (b) Wang, X.-L.; Qin, C.; Wang, E.-B.; Li, Y.-G.; Su, Z.-M.; Xu, L.; Carlucci, L. *Angew. Chem., Int. Ed.* **2005**, *44*, 5824−5827. (c) Yin, P.-X.; Zhang, J.; Li, Z.-J.; Qin, Y.-Y.; Cheng, J.-K.; Zhang, L.; Lin, Q.-P.; Yao, Y.-G. *Cryst. Growth Des.* **2009**, *9*, 4884−4896.

(8) Sheldrick, G. M. *SHELXS-97, Program for X-ray Crystal Structure Determination*; University of Gottingen: Gottingen, Germany, 1997.

(9) Sheldrick, G. M. *SHELXL-97, Program for X-ray Crystal Structure Refinement*; University of Gottingen: Gottingen, Germany, 1997.

(10) Spek, A. L. *Implemented as the PLATON Procedure, a Multipurpose Crystallographic Tool*; Utrecht University: Utrecht, The Netherlands, 1998.

(11) Liao, S.-Y.; Gu, W.; Yang, L.-Y.; Li, T.-H.; Tian, J.-L.; Wang, L.; Zhang, M.; Liu, X. *Cryst. Growth Des.* **2012**, *12*, 3927−3936.

(12) (a) Li, B.; Peng, Y.; Li, B.; Zhang, Y. *Chem. Commun.* **2005**, *18*, 2333−2335. (b) Jing, X.-H.; Yi, X.-C.; Gao, E.-Q.; Blatov, V. *Dalton Trans.* **2012**, DOI: 10.1039/C2DT31917A.

(13) (a) Dai, F.-N.; He, H.-Y.; Zhao, X.-L.; Ke, Y.-X.; Zhang, G.-Q.; Sun, D.-F. *CrystEngComm* **2010**, *12*, 337−340. (b) Su, Z.; Bai, Z.-S.; Fan,

J.; Xu, J.; Sun, W.-Y. *Cryst. Growth Des.* **2009**, *9*, 5190−5196. (c) Cheng, J.-Y.; Dong, Y.-B.; Huang, R.-Q.; Smith, M. D. *Inorg. Chim. Acta* **2005**, *358*, 891−902.
(14) Hill, R. J.; Long, D.-L.; Turvey, M. S.; Blake, A. J.; Champness, N. R.; Hubberstey, P.; Wilson, C.; Schröder, M. *Chem. Commun.* **2004**, *16*, 1792−1793.
(15) (a) He, H.-Y.; Dou, J.-M.; Li, D.-C.; Ma, H.-Q.; Sun, D.-F. *CrystEngComm* **2011**, *13*, 1509−1517. (b) Su, Y.-H.; Luo, F.; Li, H.; Che, Y.-X.; Zheng, J.-M. *CrystEngComm* **2011**, *13*, 44−46.
(16) (a) Zheng, S.-L.; Yang, J.-H.; Yu, X.-L.; Chen, X.-M.; Wong, W.-T. *Inorg. Chem.* **2004**, *43*, 830−838. (b) Yang, J.-H.; Zheng, S.-L.; Yu, X.-L.; Chen, X.-M. *Cryst. Growth Des.* **2004**, *4*, 831−836. (c) Sun, D.; Zhang, N.; Huang, R.-B.; Zheng, L.-S. *Cryst. Growth Des.* **2010**, *10*, 3699−3709.
(17) (a) Allendorf, M. D.; Bauer, C. A.; Bhaktaa, R. K.; Houka, R. J. T. *Chem. Soc. Rev.* **2009**, *38*, 1330−1352. (b) Wang, S. J.; Xiong, S.-S.; Wang, Z. Y.; Du, J. F. *Chem.—Eur. J.* **2011**, *17*, 8630−8642.
(18) (a) Zhu, Q.-L.; Shen, C.-J.; Tan, C.-H.; Sheng, T.-L.; Hua, S.-M.; Wu, X.-T. *Chem. Commun.* **2012**, *48*, 531−533. (b) Cui, Y.-J.; Yue, Y.-F.; Qian, G.-D.; Chen, B.-L. *Chem. Rev.* **2012**, *112*, 1126−1162.